

# Nanosecond Time-Resolved and Steady-State Infrared Studies of Photoinduced Decomposition of TATB at Ambient and Elevated Pressure

Elizabeth A. Glascoe,\* Joseph M. Zaug, Michael R. Armstrong, Jonathan C. Crowhurst, Christian D. Grant, and Laurence E. Fried

Lawrence Livermore National Laboratory, 7000 East Avenue, Livermore, California 94551

Received: October 23, 2008; Revised Manuscript Received: March 10, 2009

The time scale and/or products of photoinduced decomposition of 1,3,5-triamino-2,4,6-trinitrobenzene (TATB) were investigated at ambient pressure and compared with products formed at 8 GPa. Ultrafast time-resolved infrared and steady-state Fourier transform IR (FTIR) spectroscopies were used to probe TATB and its products after photoexcitation with a 5 ns pulse of 532 nm light. At ambient pressure, transient spectra of TATB indicate that the molecule has significantly decomposed within 60 ns; transient spectra also indicate that formation of CO<sub>2</sub>, an observed decomposition product, is complete within 30–40  $\mu$ s. Proof of principle time-resolved experiments at elevated pressures were performed and are discussed briefly. Comparison of steady-state FTIR spectra obtained at ambient and elevated pressure (ca. 8 GPa) indicate that the decomposition products vary with pressure. We find evidence for water as a decomposition product only at elevated pressure.

## Introduction

A microscopic understanding of the response of energetic materials to various stresses is important in the development of predictive detonation and safety models. Elucidation of the decomposition pathways of solid-state energetic materials has challenged chemists for decades because of the complex nature of the reactions and experimental limitations. Many common energetic materials have vast landscapes of decomposition pathways that change depending on the initiation process (e.g., photo, thermal, shock, and spark initiation) and initial conditions (e.g., pressure, temperature, atmosphere, sample defects, and impurities). The autocatalytic nature of some energetic material decompositions further complicate the process because the mechanism can change and accelerate as the material begins to decompose.

The molecule 1,3,5-triamino-2,4,6-trinitrobenzene (TATB) is of particular interest because of its relative stability to stresses such as heat and impact when compared with high explosives such as octahydro-1,3,5,7-tetranitro-1,3,5,7-tetrazocane (HMX), 1,3,5-trinitro-1,3,5-triazacyclohexane (RDX), and pentaerythritol tetranitrate (PETN).<sup>1</sup> The decomposition mechanism for TATB has been studied by a number of workers using a variety of experimental and theoretical methods. The first step in the decomposition mechanism remains under debate; the two most plausible mechanisms are inter/intramolecular H-atom transfer, and C–NO<sub>2</sub> bond homolysis. We consider the nitro–nitrite isomerization mechanism to be in the family C–NO<sub>2</sub> bond homolysis reactions because the mechanism involves rearrangement of the C–NO<sub>2</sub> moiety without H-atom transfer.<sup>2</sup> There is strong evidence for each mechanism, indicating that the decomposition process is complex and depends on the conditions and method of initiation.

The inter/intramolecular H-atom transfer mechanism is expected to produce H<sub>2</sub>O as well as furazan- and furoxan-derivatives of TATB. Furazan- and furoxan-derivatives and water were directly observed by Land et al. via simultaneous

thermogravimetric modulated beam mass spectrometry in isothermal heating studies.<sup>3</sup> Furazan- and furoxan-derivatives were also observed via X-ray photoelectron spectroscopy (XPS) by Sharma et al. as a byproduct debris of subignition shock and impact experiments.<sup>4</sup> Water was observed via IR spectroscopy by Makashir et al. during ramp heating experiments.<sup>5</sup> Makashir et al. also observed an early decrease in the NH<sub>2</sub> moiety population (monitored via the intensity of the N–H stretch) and attributed it to C–NH<sub>2</sub> bond cleavage; however, the population change could also be attributed to an H-atom transfer process, which should produce large vibrational frequency shifts. Rogers and co-workers studied the kinetic isotope effect in the decomposition of TATB. They documented a rate deceleration during the early stages of decomposition (i.e., before autocatalytic reactions take over) when the NH<sub>2</sub> moieties were replaced with ND<sub>2</sub>. Their results provide evidence that H-atom transfer is the rate determining step during the early stages of decomposition, although they cannot prove whether the H-atom transfer is the first step in the decomposition mechanism.<sup>6</sup> Density functional theory (DFT) calculations by Wu and Fried indicate that intramolecular H-atom transfer is the lowest barrier process, followed by intermolecular H-atom transfer and finally C–NO<sub>2</sub> bond homolysis.<sup>7</sup> In summary, there is strong evidence, based on direct experimental observation and theoretical modeling, to support the H-atom transfer mechanism and subsequent formation of H<sub>2</sub>O.

There is also strong evidence for a C–NO<sub>2</sub> bond-cleavage mechanism. DFT calculations by Wu and Fried indicate that the weakest bond in TATB is the C–NO<sub>2</sub> bond.<sup>7</sup> Sharma et al. directly observed a decrease in the NO<sub>2</sub> population via XPS after UV irradiation, subignition shocks, and thermal damage.<sup>4,8,9</sup> Their UV irradiation studies reveal depletion of the NO<sub>2</sub> population exclusively and they observed no evidence for any other decomposition mechanism.<sup>8,9</sup> In contrast, their thermal and subignition shock experiments indicate that the C–NO<sub>2</sub> mechanism is dominant yet the H-atom transfer mechanism also occurs.<sup>4,8,9</sup> Kakar et al. compared the electronic structure of TATB before and after intense white light irradiation and found clear evidence for depletion of NO<sub>2</sub> groups in the radiation-

\* To whom correspondence should be addressed: E-mail: glascoe2@llnl.gov.

damaged material.<sup>10</sup> Brill et al. measured the evolved products during high-temperature isothermal heating experiments using Fourier transform infrared spectroscopy (FTIR) and found little to no H<sub>2</sub>O formation and deduced that the decomposition began with C–NO<sub>2</sub> bond homolysis.<sup>11</sup> In this work, Brill also summarized the relevant literature and hypothesized that, under slow heating, the low barrier process of inter/intramolecular H-atom transfer may be the dominant channel, whereas more aggressive heating to higher temperatures may favor cleavage of the C–NO<sub>2</sub> bond.<sup>11</sup>

Photoinduced decomposition pathways for TATB have not been studied as extensively as thermal or shock-induced decomposition. In general, photoexcitation of a molecule will populate an excited state that can typically proceed down two different pathways: (1) internal conversion back to the ground state with a high degree of vibrational energy, or (2) internal conversion or intersystem crossing to another excited state from which the molecule may return to the ground state or couple to a dissociative state resulting in a chemical reaction.<sup>12</sup> In the first scenario, the molecule may be in a state that is similar to that resulting from rapid heating. In the second scenario, it may induce a chemical mechanism that is unique and unlike the thermal pathway. The advantage of photoinduced decomposition is that the nonequilibrium population can be formed on the same time scale as the pulse duration of the light.

Of the existing photoinduced studies of TATB, only Sharma et al.<sup>8,9</sup> and Kakar et al.<sup>10</sup> attempted to characterize the mechanism based on the products after UV irradiation, whereas the other studies focused on reaction rates. In a study by Peiris et al., the photoinduced rate of decomposition was monitored as a function of static pressure between ambient and 2 GPa.<sup>13</sup> Peiris concluded that the induction time for decomposition was pressure independent and that the rate of decomposition increased with pressure.<sup>13</sup> These results are consistent with Foltz's study of the pressure-dependent reaction propagation rate of photoinduced TATB.<sup>14</sup> Foltz found that the reaction propagation rate increases linearly with pressure between ambient pressure and 18.4 GPa. Between 18.4 and 40 GPa, there are two discontinuities in the reaction propagation rate.<sup>14</sup> In contrast, Geifers and Pravica found that the TATB decomposition rate decreased as a function of pressure when subjected to X-ray radiation.<sup>15</sup> These studies provide a global understanding of the sensitivity of TATB to photo- and radiation-induced damage; Sharma's<sup>8,9</sup> and Kakar's<sup>10</sup> studies provide insight into a potential mechanism and both indicate that C–NO<sub>2</sub> bond cleavage is the primary decomposition pathway upon photoexcitation. On the basis of the static pressure, diamond anvil cell studies,<sup>13–15</sup> it is evident that the decomposition rate changes as a function of pressure and yet no detailed mechanism has been suggested for elevated pressures.

In an effort to elucidate the photoinduced decomposition mechanism of TATB, we have experimentally measured the parent decomposition and product formation kinetics at ambient pressure using time-resolved infrared spectroscopy and compared ambient and elevated pressure (ca. 8 GPa) pre- and postphotolysis spectra using steady-state FTIR spectroscopy. The decomposition process was photoinduced using a 5 ns pulse of 532 nm light. Transient infrared spectra were collected at various times (up to 80  $\mu$ s) after photoexcitation using a  $\sim$ 50 fs pulse of broadband infrared light. Equilibrium product spectra were collected within a few minutes after photoexcitation, and the products of ambient and elevated pressures were compared.

The results of the ambient pressure studies indicate that the decomposition process occurs on the nanosecond time scale,

and final product formation occurs within tens of microseconds. Under ambient initial pressure and using the photoexcitation parameters above, water was not observed in either the transient spectra or the equilibrium product spectra. At elevated pressures, water was observed as an equilibrium product. These results provide direct evidence that the mechanism of photoinduced TATB decomposition changes dramatically as the pressure is elevated and indicate that the debated water-formation mechanism is, in part, dependent on the initial pressure. Possible reasons for this will be suggested.

## Experimental Section

**Sample.** TATB powder synthesized at LLNL was ground to a uniform grain size of 1  $\mu$ m (LLNL Lot C-090, purchased from Mason and Hanger prepared via the dry-aminated method). For the ambient pressure experiments, the sample was compressed to a thickness of 3–5  $\mu$ m between two IR-grade CaF<sub>2</sub> windows.<sup>16</sup> A typical sample provided enough area for ca. 100–400 laser shots. Results of experiments performed with different sample/window assemblies on different days indicate that variability due to sample preparation was minimal.

For high-pressure measurements, a diamond anvil cell (DAC) was employed. The DAC sample cavity comprises two counter-opposed 400  $\mu$ m diameter type Ia diamond culets and a preindented 50  $\mu$ m thick Re foil gasket. The chamber diameter is cut using a micro electric discharge machine purchased from Hylozoic Products and is nominally 225  $\mu$ m. Cesium iodide is compressed into the sample chamber to transmit applied pressure and provide thermal insulation between TATB and the diamond windows; strontium tetraborate was used as a pressure manometer.<sup>17</sup>

**Instrumentation.** Both the ambient- and high-pressure samples were photoinitiated (i.e., pumped) with a 5 ns pulse (fwhm) of 532 nm light and probed with a 50 fs pulse (fwhm) of tunable mid-IR light. The time delay between the pump and the probe was varied from shot to shot to resolve the dynamics of the parent molecule and product species as a function of time. Micro-FTIR spectra were collected within 10 min of pumping to characterize the equilibrium products of decomposition.

In the case of the pump pulse, 532 nm light, (the second harmonic of a Nd:YAG laser - New Wave Research, Polaris II 20 MHz), was focused to a fwhm diameter of ca. 59  $\mu$ m. As the sample thickness in the ambient pressure experiments varied from one experiment to the next, the laser power was adjusted to achieve a complete decomposition of the irradiation site; the laser fluence was typically  $20 \pm 5$  J/cm<sup>2</sup>. In the high-pressure experiments, significantly less power was required to induce photodecomposition;<sup>14</sup> consequently, the laser fluence was ca. 7 J/cm<sup>2</sup>.

The micro-FTIR measurements were used to characterize the equilibrium products of photoinduced TATB. A 580–8000 cm<sup>-1</sup> spectrum was collected ca. 10 min after photoexcitation; a detailed description of the instrument was provided previously.<sup>18</sup> A mid-IR glow bar source is focused to a diameter of ca. 1 mm, transmitted through a sample, and focused into a cryogenically cooled single element InSb–HgCdTe sandwich detector. Two irises are situated along the beam path before and after the sample to enable  $>30$   $\mu$ m spatially resolved IR absorption measurements; however, we typically used larger spot sizes to increase our signal-to-noise ratio. A Bruker Optics Vector 33 interferometer is used to collect preselected 2 cm<sup>-1</sup> resolution data. Background spectra of the window absorption are collected prior to loading samples.

Time resolved infrared spectroscopy (TRIR) was employed to monitor the TATB reaction process upon photoexcitation. This technique entails generating ultrafast infrared (IR) light by pumping a mid-IR optical parametric amplifier (OPA) (Coherent, Opera) with the output of a Ti-Sapphire amplifier (Coherent, Mira) that is seeded by a Ti-Sapphire oscillator (Coherent, Legend). Typically, the OPA is pumped by a 1 kHz train of 50 fs pulses with an average power of 1 mJ/pulse and a central wavelength of 800 nm and generates a 1 kHz train of pulses tunable from 1000–5000  $\text{cm}^{-1}$  with a typical bandwidth of 300  $\text{cm}^{-1}$  at 3000  $\text{cm}^{-1}$ , an average power of 2  $\mu\text{J}/\text{pulse}$ , and an average pulse duration of 50 fs. IR pulses are focused through an alignment iris by a gold-coated off-axis optical parametric mirror ( $f_l = 100$  mm) and directed into a Cassegrain objective (Newport Optics; Al surface, 15 $\times$  magnification, numerical aperture = 0.4, field of view = 1.2 mm, focal length = 13 mm). We selected this objective to focus the IR beam down to a 15–20  $\mu\text{m}$  diameter fwhm spot size; the size of DAC samples are typically less than 50  $\mu\text{m}$  in diameter. A second, identical Cassegrain objective collects the transmitted light and focuses it through a second spatial alignment iris. Finally, the beam is focused, using a gold-coated off-axis optical parametric mirror ( $f_l = 45$  mm), into a spectrograph (Jobin Yvon, iHR320), and detected using a 64 element cryogenically cooled HgCdTe (MCT) infrared-array detector (InfraRed Associates, Inc.) and a high-speed signal acquisition system and software (Infrared Systems Development Corp.). The wavenumber resolution of this system, using a 58 grooves/mm grating, is 3  $\text{cm}^{-1}/\text{pixel}$  at 3000  $\text{cm}^{-1}$  and 0.5  $\text{cm}^{-1}/\text{pixel}$  at 1400  $\text{cm}^{-1}$ . To minimize loss of signal, all optics within the spectrograph are gold coated.

For single-shot time-resolved experiments, a digital delay system triggers the 532 nm pump laser and synchronizes the IR pulse with the detector electronics. Because of the pulse duration of the 532 nm photoexcitation laser, the time resolution for these studies was limited to  $>5$  ns. Time zero ( $t_0$ ) was roughly established by monitoring the parent molecule depletion<sup>19</sup> of  $[\text{CpW}(\text{CO})_3]_2$  in neat  $\text{CH}_2\text{Cl}_2$  and fine-tuned using the average initiation of photodepletion in the TATB.<sup>20</sup>

## Results and Discussion

**I. Ambient Pressure Results.** Ambient pressure experiments were performed with a single-window and a double-window configuration. In the double window experiments, TATB was sandwiched between two  $\text{CaF}_2$  windows and the photoproduct gases were trapped in the reaction volume. In the single window experiments, the TATB was mounted on a single  $\text{CaF}_2$  window so that product gases were able to escape. By doing both experiments, we were able to explore the possibility of trapped gases autocatalyzing the decomposition of TATB.

In both the single- and double-window experiments, photoexcitation of TATB results in the formation of a small hole where the laser impinged on the sample; visual inspection shows only a dusting of residual black material on the windows. Comparison of pre- and postphotolysis  $\mu$ -FTIR spectra from the double-window sample (part a of Figure 1) show depletion of the TATB peaks and formation of products. The postphotolysis spectrum indicates that there is a small population of residual TATB, which is attributed to the material at the edge of the photolysis hole. Three product peaks are observed in the postphotolysis spectrum at 2345, 2172, and 2094  $\text{cm}^{-1}$ . The 2345  $\text{cm}^{-1}$  peak is assigned to  $\text{CO}_2$  based on its vibrational frequency and its observation as a TATB thermal decomposition product in a variety of studies;<sup>3,5,11,21–23</sup> the 2172  $\text{cm}^{-1}$  peak is assigned to CO for the same reasons.<sup>3,11,21–23</sup> The peak at 2094

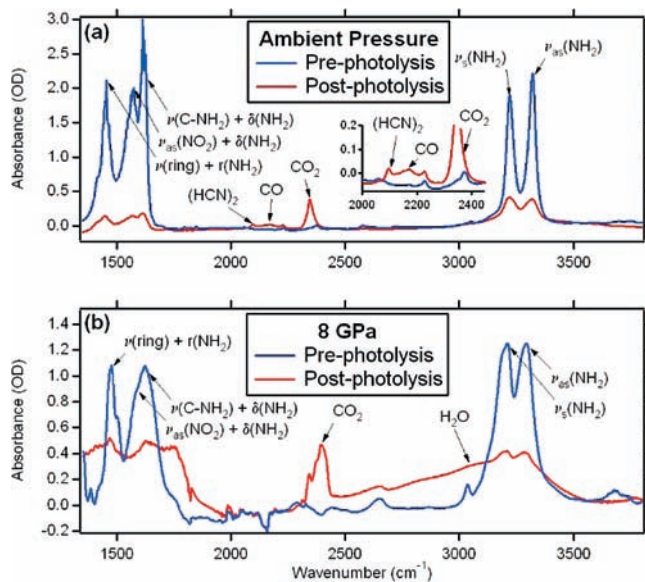


**Figure 1.** Steady-state FTIR spectra of pre- and postphotolysis TATB at (a) ambient pressure (using a double window configuration to trap evolved gases) and (b) 8 GPa (in a diamond anvil cell).

$\text{cm}^{-1}$  corresponds to a  $\text{C}\equiv\text{C}$ , CN, or CO vibration based on comparisons with generic functional-group frequencies. While this peak could not be definitively identified, it may be a derivative of HCN, a common product of TATB decomposition,<sup>3,5,11,21</sup> and, indeed, the vibrational frequency matches that of  $(\text{HCN})_2$ .<sup>24</sup> Other products are difficult to characterize due to spectral congestion (e.g.,  $\text{NH}_3$ ) or IR inactive vibrations (e.g.,  $\text{O}_2$ ,  $\text{H}_2$ , and  $\text{N}_2$ ). There are, however, a number of studies that have explored the products of TATB decomposition.<sup>3–5,11</sup>

The photoinduced decomposition kinetics of TATB were investigated by monitoring the spectral changes at three distinct spectral regions providing information about the  $\text{NO}_2$  and  $\text{NH}_2$  moieties and the TATB ring.<sup>25,26</sup> Transient absorption spectra presented in Figure 2 were generated by normalizing the transient transmission spectrum by its corresponding prephotolysis transmission spectrum. Negative peaks result from photodepleted starting material (i.e., TATB) and positive peaks result from transient or product species. Figure 2 shows the photodepletion or bleach spectra of the symmetric  $\text{NH}_2$  vibration (part a of Figure 2), the asymmetric  $\text{NO}_2$  vibration (part b of Figure 2), and the ring stretch (part c of Figure 2) upon excitation with 532 nm in the single-window configuration. Figure 3 displays the bleach dynamics of all three of the peaks in the single-window configuration. Figure 4 displays the bleach dynamics of all three peaks in the double-window configuration (overlaid with the single window results). The data points in Figures 3 and 4 correspond to individual experiments and the solid lines provide the average, long-time (ca. minutes) amplitude for bleaching. In both single- and double-window configurations, the ring-vibration appears to be depleted instantaneously and is assigned a depletion time of  $\leq 10$  ns. In contrast, the  $\text{NO}_2$  and  $\text{NH}_2$  vibrations both appear to reach equilibrium at ca. 60 ns.

There are two possible interpretations of the IR absorption dynamics presented in Figures 3 and 4. The first is that the ring is broken apart within 10 ns of photoexciting TATB, resulting in ring fragments with unperturbed  $\text{NO}_2$  and  $\text{NH}_2$  groups. The initiation mechanism of ring fission has been observed only once before in TATB by Farber and Srivastava; their experiment involved thermal decomposition of TATB and product detection

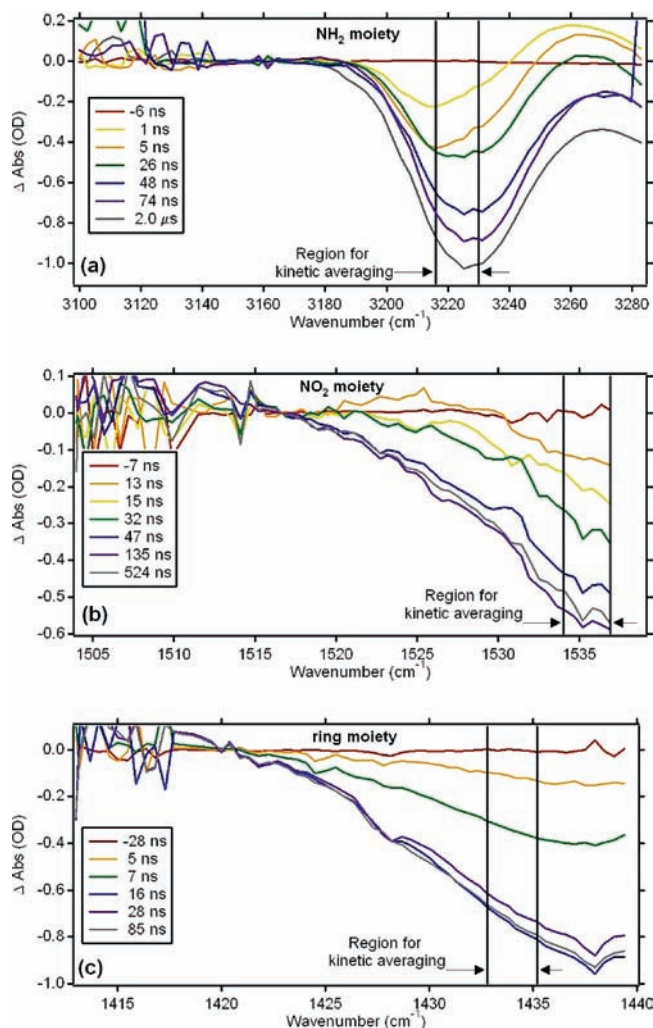


**Figure 2.** Transient spectra collected as a function of time after photoexcitation of TATB at ambient pressure in the single-window configuration showing photodepletion of the (a)  $\text{NH}_2$  moiety, (b)  $\text{NO}_2$  moiety, and (c) ring. Data between the black lines was averaged and plotted as a function of time in Figure 3.

via mass spectrometry.<sup>22</sup> However, no other TATB decomposition study found any evidence for ring fragmentation as the primary decomposition step, regardless of the initiation method (i.e., thermal, photo, impact, or shock).<sup>3–6,8,9,11</sup> In the case of our photoinduced decomposition mechanism, one could argue that the excited state populated by photoexcitation of TATB may access a facile pathway to ring fragmentation. However, an experimental study of the electronic structure of TATB by Kakar et al. indicates that the UV excitation of TATB results in a charge transfer from the  $\text{NH}_2$  group to the  $\text{NO}_2$  group and white light irradiation of TATB results in ejection of the  $\text{NO}_2$  substituent from the molecule with no evidence for ring fission.<sup>10</sup> Similarly, photoexcitation of simpler aromatic systems (i.e., benzene, nitrobenzene, and aniline) demonstrate the stability of the aromatic ring. Ring cleavage in photoexcited benzene is a low quantum yield process (ca. 0.01–0.05)<sup>27,28</sup> and photoexcitation of nitrobenzene and aniline favor reactions at the  $\text{NO}_2/\text{NH}_2$  moiety rather than ring cleavage.<sup>29–31</sup> Although we cannot rule out the possibility of ring fission as the primary decomposition step in TATB, it seems unlikely based on the stability of the aromatic ring and on the limited observations of ring fission in other TATB decomposition studies.<sup>3–6,8,9,11</sup>

The more plausible interpretation of the IR absorption dynamics presented in Figures 3 and 4 is that the ring is

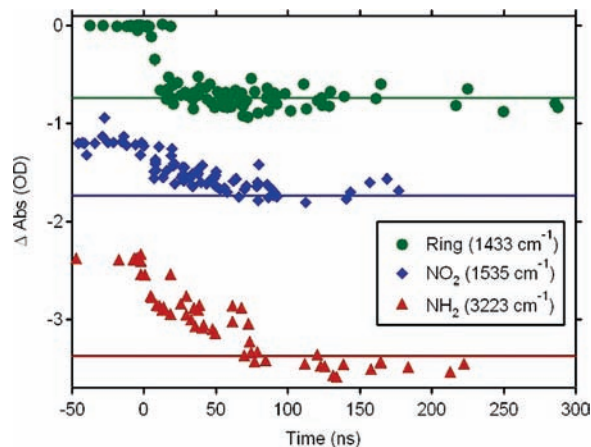


**Figure 3.** Dynamics of TATB absorption after photoexcitation in an ambient pressure, single-window configuration;  $\text{NO}_2$  and  $\text{NH}_2$  data sets (blue and red data respectively) were manually shifted down from zero OD by 1.2 and 2.4 OD, respectively. Data points represent individual experiments; the solid lines represent the average long-time-delay absorption collected a few minutes after photoexcitation.

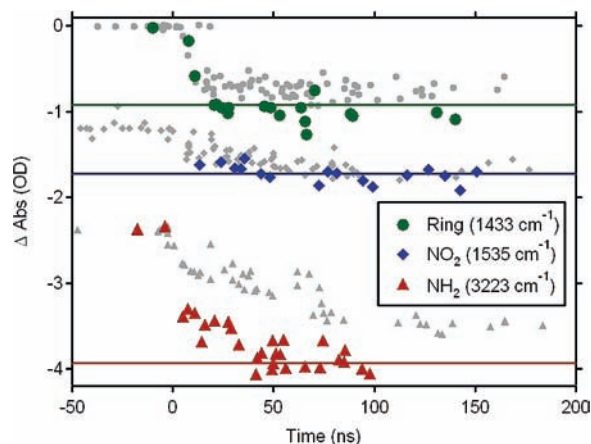


**Figure 4.** Dynamics of TATB absorption after photoexcitation in an ambient pressure, double-window configuration;  $\text{NO}_2$  and  $\text{NH}_2$  data sets (blue and red respectively) were manually shifted down from zero OD by 1.2 and 2.4 OD, respectively. Data points represent individual experiments; solid line represents the average long-time-delay absorption collected a few minutes after photoexcitation. Gray points represent the respective single-window data from Figure 3.

sufficiently distorted via photoexcitation so that its vibrational frequency shifts out of the spectral probe region. In this scenario, the ring would remain intact initially despite the disappearance of its IR peaks and break apart later in the decomposition mechanism. Consequently, the  $\text{NO}_2$  and  $\text{NH}_2$  vibrational frequencies would serve as the best indicators for the decomposition of TATB. One can think of a number of different scenarios in which the ring can be altered, for example ring structure rearrangement<sup>28</sup> or homolytic cleavage of a single  $\text{NO}_2$  or  $\text{NH}_2$  group from the ring, and so forth. These results provide the first evidence that photoinduced decomposition of TATB occurs on the nanosecond time scale.

Of the product species observed in the double-window  $\mu$ -FTIR measurements, only the  $\text{CO}_2$  peak at  $2345\text{ cm}^{-1}$  was sufficiently intense to monitor using the TRIR system. Absorption spectra at a variety of delay times, ranging from 0.4 to 80  $\mu\text{s}$ , after excitation with 532 nm light are shown in Figure 5. The time-dependent evolution of the peak at  $2345\text{ cm}^{-1}$  (shown in Figure 6) indicates that  $\text{CO}_2$  reaches equilibrium at 30–40  $\mu\text{s}$ .

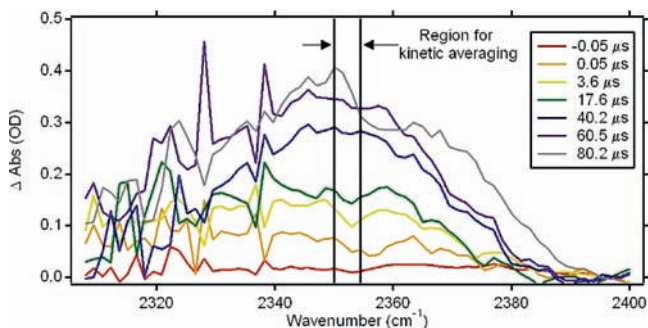


**Figure 5.** Transient product absorption spectra collected after photoexcitation of TATB at ambient pressure in the double-window configuration. The product peak is assigned to the asymmetric stretch of  $\text{CO}_2$ .

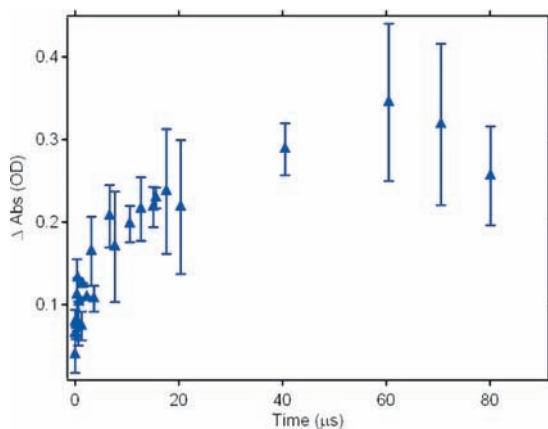


**Figure 6.** Optical absorption of  $\text{CO}_2$  as a function of time based on the amplitude of the  $2345\text{ cm}^{-1}$  peak.

Most notably absent in our product spectra are any peaks that could be assigned to water. To irrevocably prove the absence of water, one would need a complete knowledge and balance of all reactant and product concentrations. However, a reactant/product balance analysis of our data is not feasible as some possible products are infrared inactive (e.g.,  $\text{N}_2$ ,  $\text{O}_2$ ,  $\text{H}_2$ , etc.) and other products are difficult to characterize due to spectral congestion (e.g.,  $\text{NH}_3$ ). The absence of any water peaks, specifically the absence of a peak at ca.  $3350\text{ cm}^{-1}$ , indicates that either the concentration of water is extremely low (i.e., significantly less than that observed in the elevated pressure experiments), the water has reacted with the  $\text{CaF}_2$  windows, or has diffused away from the FTIR probe region. Previous studies indicate that  $\text{CaF}_2$  is inert to water under our conditions and, in the most extreme cases,<sup>32</sup>  $\text{CaF}_2$  adsorbs  $\text{OH}^-$  ions that would be apparent in our FTIR spectra. If water were to diffuse away, then we might observe water in the transient spectra. In addition, one would expect  $\text{CO}_2$  to also diffuse away, yet it remains trapped in the reaction space. Whereas we cannot indisputably prove the absence of water, the concentration, if formed at all, is significantly less than that observed in the elevated-pressure experiments, therefore, it is estimated effectively absent.

On the basis of our measurements of TATB photodepletion and  $\text{CO}_2$  product formation time scales; it is evident that the photoinduced chemistry of TATB occurs on the nanosecond to microsecond time scale. The time-dependent temperature profile is a potentially important parameter but is difficult to determine because assessing the initial temperature after photoexcitation requires a complete knowledge of the excitation and energy dissipation mechanisms. The initial temperature was estimated using the conservation of energy and assuming all of the energy

input into the system is converted into heat; we calculate a temperature on the order of hundreds of degrees Celsius depending on the fraction of light absorbed. The time scale for heat loss can be estimated from the thermal conductivity of the poorest thermal conducting material (i.e., TATB in all scenarios).<sup>33</sup> This time scale for thermal diffusion is greater than  $10\ \mu\text{s}$  and thus much longer than the initiation reactions.

**II. Elevated Pressure Results.** Proof of principal TRIR and  $\mu$ -FTIR experiments of TATB in a diamond anvil cell were performed. Photoexcitation of TATB at 8 GPa consistently produced a black residue and often burned much more material than the irradiated portion. Part b of Figure 1 displays the pre- and postphotolysis  $\mu$ -FTIR spectra of the sample at 8 GPa. Two product peaks are observed in the postphotolysis spectrum.<sup>34</sup> The peak at  $\sim 2395\text{ cm}^{-1}$  is assigned to  $\text{CO}_2$  based on its peak position and previous observations of  $\text{CO}_2$  as a decomposition product of TATB.<sup>3,5,11,21–23</sup> The  $50\text{ cm}^{-1}$  blue shift in the  $\text{CO}_2$  peak position relative to the ambient-pressure peak position is consistent with previous pressure-dependent IR studies of  $\text{CO}_2$ .<sup>35</sup> The broad peak at  $3100\text{ cm}^{-1}$  is assigned to  $\text{H}_2\text{O}$  based on the pressure-dependent position and broad shape. A comparison of multiple 8 GPa pre- and postphotolysis spectra indicates that the relative concentration of  $\text{H}_2\text{O}$  is variable (Supporting Information). One possible explanation for the population variability is discussed in part IV.

A comparison of the ambient and elevated pressure postphotolysis spectra in parts a and b of Figure 1 indicates that the formation of  $\text{H}_2\text{O}$  is pressure dependent. Over 30 different ambient pressure experiments were analyzed using the  $\mu$ -FTIR and none show any evidence for water formation. In addition, the ambient pressure time-resolved experiments show no evidence for water formation on the nanosecond to microsecond time scale. In contrast, high-pressure time-resolved studies of the water region (ca.  $3000\text{ cm}^{-1}$ ) of the spectrum between 1 and  $5\ \mu\text{s}$  show erratic spectral changes in which some transient spectra clearly show water formation and others indicate that water formation has not begun at these times. Extrapolation of our high-pressure results in which transient water was observed indicates that water formation equilibrates on the 5–65 microsecond time scale. Similarly, measurements at the  $\text{CO}_2$  region of the spectrum at ca.  $2.3\ \mu\text{s}$  indicate that  $\text{CO}_2$  begins to form on a time scale that may be similar to that measured at ambient pressure (refer to Figure 6). Further work is necessary to establish the formation time of  $\text{H}_2\text{O}$  and  $\text{CO}_2$  at elevated pressures.

**III. Discussion of Mechanism of Photoexcitation.** The physical response mechanisms of a photoinduced event will depend on the material, the wavelength, the energy, and the duration of the light pulse. In the case of TATB, the sequence following photolysis is still poorly understood. A common question is whether the photoinduced reactions in TATB are induced by a single photon or multiple photons. The electronic absorption spectrum of solid TATB between 280 and  $430\text{ nm}$  shows a strong absorption at  $370\text{ nm}$  that tails off to ca. 50% at  $430\text{ nm}$ .<sup>13</sup> The single photon absorption cross-section at  $532\text{ nm}$  is expected to be weak; however, studies of other materials indicate that despite a small absorption cross section, a high-power light pulse can still create a measurable population of photoproducts via single photon excitation.<sup>36</sup> Recent work by Kunz et al. indicates single photon photoinitiation occurs at crystal dislocations and defects in an energetic material; these dislocations are enhanced with the application of pressure resulting in an increased photosensitivity with pressure.<sup>37</sup> In our ambient pressure experiments, preparation of the sample

involved grinding and compressing the TATB powder until a thin uniform layer was generated. Presumably this process dramatically increased the crystal dislocations or defects making the single photon absorption cross section increase in the visible. Preparation of our samples for our high-pressure experiments may not have introduced more dislocations but the elevated pressure will increase the single photon absorption cross section in the visible region.<sup>37</sup> It is, however, not clear to us, based on our studies, whether the observed decomposition of TATB involves a single or multiphoton process.

**IV. Discussion of the Mechanistic Interpretation of Results.** Comparison of our ambient- and elevated-pressure results indicates that the photoinduced decomposition mechanism is pressure dependent. The presence of water in the decomposition products of 8 GPa TATB provides a clue to the mechanism of decomposition. The first step in the thermal decomposition of TATB is expected to involve either inter/intramolecular H-atom transfer and subsequent formation of H<sub>2</sub>O, or C–NO<sub>2</sub> bond homolysis and limited H<sub>2</sub>O formation. Brill and James hypothesized that the thermal heating rate will favor one channel over the other: rapid heating to high temperatures will favor C–NO<sub>2</sub> bond homolysis, whereas slow heating will favor H-atom transfer.

Photoexcitation of a material will populate an excited state that can either couple to a reaction pathway, resulting in chemical reactions, or undergo internal conversion back to the ground state of the starting molecule. The latter scenario results in a vibrationally excited (i.e., hot) ground electronic state parent molecule that is expected to be similar to a molecule excited via rapid, high-temperature heating. In turn, this vibrationally excited molecule can undergo thermally induced reactions similar to those expected from rapid, high-temperature heating experiments; therefore, it is reasonable to draw comparisons between a photoinduced reaction and a high-temperature, rapid heating experiment. The fact that previous photodecomposition experiments and rapid heating experiments all propose the same decomposition mechanism reinforces our claim that it is reasonable to compare the two experiments.<sup>8–11</sup> The absence of water in our ambient-pressure experiments is consistent with Brill and James's hypothesis and experimental observations.<sup>11</sup>

In contrast to our ambient pressure experiments, our elevated-pressure photoexcitation produced water, indicating that pressure may facilitate the H-atom abstraction or that pressure may inhibit the C–NO<sub>2</sub> bond homolysis process. In addition, photoexcitation of TATB at 8 GPa often burned much more material than the irradiated portion. This was quite different from the ambient-pressure experiments in which only the irradiated portion reacted, indicating that pressure changes the reaction. If the temperature of the TATB were the main variable determining whether a burn propagates, one would expect the better-insulated sample to burn more. In our experiments, the better insulated, i.e. the ambient-pressure experiments, display little or no burn propagation. Thus, the response of TATB to photoinitiation is more complex than simply a temperature difference and one of the main variables is the preinitiation pressure, as indicated by our study and the work of others.<sup>13,14</sup>

We suggest two interpretations of our results. Either the initiation mechanisms at the two pressures are different, or the initiation mechanisms are the same and the observed reactivity difference between the two pressures is caused by the subsequent reaction propagation. In the first scenario, elevated pressure may inhibit the formation of C–NO<sub>2</sub> bond homolysis and therefore block the primary, high-temperature, decomposition mechanism. Alternatively, the phase (i.e., liquid vs gas) of the initial

decomposition products at ambient and elevated pressure may change the autocatalytic decomposition mechanism. We cannot assess the degree to which these processes cocontribute to the final products' formation.

In the second scenario, the elevated-pressure and ambient-pressure decompositions have the same laser initiation mechanism (i.e., C–NO<sub>2</sub> bond cleavage), which produces little or no water. The subsequent reaction propagation of TATB (i.e., the burn), which is only observed at elevated pressures above a few GPa,<sup>14</sup> may access the water formation pathway. In other words, the ambient pressure final FTIR spectrum only represents a single reaction type (C–NO<sub>2</sub> bond cleavage), whereas the elevated pressure reaction represents two steps: the laser initiation step (C–NO<sub>2</sub> bond cleavage) and the propagation step (H-atom transfer and H<sub>2</sub>O formation). In this scenario, the erratic appearance of water in the transient spectra (in the time frame monitored) and variable concentration in the FTIR spectra may occur because the change in mechanism from initiation to burn may vary with the sample dimensions (i.e., total sample size, thickness in irradiation zone, amount of sample not irradiated, etc.).

This second hypothesis allows for a possible answer to the question: why does the decomposition of TATB propagate at elevated pressures but not ambient pressure?<sup>14</sup> The answer may be that the initiation step, involving furoxan- and furazan-derivative formation, may be too high at ambient pressure for the TATB deflagration to sustain propagation; however, at elevated pressures the barrier to furoxan- and furazan-derivative formation may decrease and consequently facilitate a propagation of the reaction. Further work is necessary to establish whether this hypothesized mechanism is correct.

**V. Summary.** We have demonstrated the feasibility of performing nanosecond time-resolved IR absorption studies on reacting samples at gigapascal pressures using a diamond anvil cell. Time-resolved IR measurements enabled the interrogation of energetic material solids during decomposition. We investigated the photoinduced decomposition of TATB at ambient pressure and 8 GPa. Ambient-pressure results indicate that the decomposition of TATB occurs on the nanosecond time scale where final product formation is complete ca. 30–40 microseconds after photoexcitation. Both transient and steady-state spectra at ambient pressure indicate no water formation during or upon completion of the decomposition reaction. In contrast to this finding, steady-state spectra at 8 GPa reveal a small but consistent population of water after photoexcitation. Pressure clearly affects the mechanism of TATB decomposition. Additional work is necessary to better determine the intermediate steps governing the decomposition of TATB.

**Acknowledgment.** This work performed under the auspices of the U.S. Department of Energy by Lawrence Livermore National Laboratory under Contract DE-AC52-07NA27344. The project 06-SI-005 was funded by the Laboratory Directed Research and Development Program. We thank J. L. Maienschein for kindly providing the Polaris laser used in this study, P. F. Pagoria for providing TATB samples, and Jack Reaugh for helpful discussion.

**Supporting Information Available:** Pre- and post-photolysis FTIR spectra of TATB at elevated pressure. This material is available free of charge via the Internet at <http://pubs.acs.org>.

## References and Notes

- (1) Meyer, R.; Kohler, J.; Homburg, A. *Explosives; Fifth, Completely Revised Edition*, Fifth ed.; Wiley-VCH: Weinheim, 2002.

- (2) Brill, T. B.; James, K. J. *Chem. Rev.* **1993**, *93*, 2667.
- (3) Land, T. A.; Siekhaus, W. J.; Foltz, M. F.; Behrens, R., Jr. In *Proceedings of the Tenth International Detonation Symposium*, Boston, MA, 1993; Short, J. M., Ed.; Office of Naval Research: Arlington, VA, 1993; p 181.
- (4) Sharma, J.; Forbes, J. W.; Coffey, C. S.; Liddiard, T. P. *J. Phys. Chem.* **1987**, *91*, 5139.
- (5) Makashir, P. S.; Kurian, E. M. *J. Therm. Anal.* **1996**, *46*, 225.
- (6) Rogers, R. N.; Janney, J. L.; Einger, M. H. *Thermochim. Acta* **1982**, *59*, 287.
- (7) Wu, C. J.; Fried, L. E. *J. Phys. Chem.* **2000**, *104*, 6447.
- (8) Sharma, J.; Garrett, W. L.; Owens, F. J.; Vogel, V. L. *J. Phys. Chem.* **1982**, *86*, 1657.
- (9) Sharma, J.; Owens, F. J. *Chem. Phys. Lett.* **1979**, *61*, 280.
- (10) Kakar, S.; Nelson, A. J.; Treusch, R.; Heske, C.; van Buuren, T.; Jimenez, I.; Pagoria, P.; Terminello, L. *J. Phys. Rev. B* **2000**, *62*, 15666.
- (11) Brill, T. B.; James, K. J. *J. Phys. Chem.* **1993**, *97*, 8752.
- (12) Atkins, P. *Physical Chemistry*, 6th ed.; W.H. Freeman and Co.: New York, 1998.
- (13) Peiris, S. M.; Pangilinan, G. I.; Russell, T. P. *Proceedings of the Conference of the American Physical Society Topical Group on Shock Compression of Condensed Matter*, Snowbird, UT, June 27–July 2, 1999; Furnish, M. D., Chhabidas, L. C., Hixson, R. S., Eds.; AIP Conference Proceedings, Melville, NY, 2000; p 451, 2000.
- (14) Foltz, M. F. *Propellants, Explosives, Pyrotechnics* **1993**, *18*, 210.
- (15) Geifers, H.; Pravica, M. *J. Phys. Chem. A* **2008**, *112*, 3352.
- (16) Sample thickness determined using white-light interferometry.
- (17) Datchi, F.; LeToullec, R.; Loubeyre, P. *J. Appl. Phys.* **1997**, *81*, 3333.
- (18) Montgomery, W.; Zaug, J. M.; Howard, M. H.; Goncharov, A. F.; Crowhurst, J. C.; Jeanloz, R. *J. Phys. Chem. B* **2005**, *109*, 19443.
- (19) Cahoon, J. F.; Kling, M. F.; Sawyer, K. R.; Frei, H.; Harris, C. B. *J. Am. Chem. Soc.* **2006**, *128*, 3152.
- (20) Fine adjustment involved subtracting 44 ns. As the photodepletion of ring at 1433  $\text{cm}^{-1}$  displayed an instantaneous drop in amplitude, which is a common indicator of a process that occurs on a faster timescale than the detection limit, this fine adjustment was deemed necessary and acceptable.
- (21) Brill, T. B.; Brush, P. J.; James, K. J.; Shepherd, J. E.; Pfeiffer, K. J. *Appl. Spectrosc.* **1992**, *46*, 900.
- (22) Farber, M.; Srivastava, R. D. *Combust. Flame* **1981**, *42*, 165.
- (23) Quenneville, J.; Germann, T. C.; Kober, E. M. *Proceedings of the Conference of the American Physical Society Topical Group on Shock Compression of Condensed Matter*, Waikoloa, Hawaii, June 24–29, 2007; Elert, M., Furnish, M. D., Chau, R., Holmes, N. C., Nguyen, J., Eds.; AIP Conference Proceedings, Melville, NY, 2000; p 451.
- (24) Jones, W.; Seel, R.; Sheppard, N. *Spectrochim. Acta* **1969**, *25A*, 385.
- (25) Huang, Z.; Chen, B.; Gao, G. *J. Mol. Struct.* **2005**, *752*, 87.
- (26) Liu, H.; Zhao, J.; Ji, G.; Wei, D.; Gong, Z. *Phys. Lett. A* **2006**, *358*, 63.
- (27) Worth, G. A. *J. Photochem. Photobiol., A* **2007**, *190*, 190.
- (28) Bryce-Smith, D.; Gilbert, A. *Tetrahedron* **1976**, *32*, 1309.
- (29) He, Y.; Gahlmann, A.; Feenstra, J. S.; Park, S. T.; Zewail, A. H. *Chem. Asian. J.* **2006**, *1–2*, 56.
- (30) Hurley, R.; Testa, A. C. *J. Am. Chem. Soc.* **1967**, *89*, 6917.
- (31) Saito, F.; Tobita, S.; Shizuka, H. *J. Photochem. Photobiol., A* **1997**, *106*, 119.
- (32) Lehmann, A.; König, G.; Rieder, K. H. *Chem. Phys. Lett.* **1995**, *235*, 65.
- (33) Carslaw, H. S.; Jaeger, J. C. *Conduction of Heat in Solids*, 2nd edition ed.; Clarendon Press: Oxford, 1959.
- (34) Because of strong type Ia diamond absorptions at 1950–2200  $\text{cm}^{-1}$ , the existence of CO in the product population could not be determined.
- (35) McCluskey, M.; Hsu, L.; Wang, L.; Haller, E. *Phys. Rev. B* **1996**, *54*, 8962.
- (36) Glascoe, E. A.; Kling, M. F.; Shanoski, J. E.; Harris, C. B. *Organometallics* **2006**, *25*, 775.
- (37) Kunz, A. B.; Kuklja, M. M.; Botcher, T. R.; Russell, T. P. *Thermochim. Acta* **2002**, *384*, 279.